Journal of Aerosol Science 105 (2017) 73–83

Contents lists available at ScienceDirect

Journal of Aerosol Science

journal homepage: www.elsevier.com/locate/jaerosci

Effects of organic aerosol loading and fog processing on organic aerosol volatility

Abhishek Chakraborty[a], S.N. Tripathi[a,b,*], Tarun Gupta[a,b,*]

[a] Department of Civil Engineering Indian Institute of Technology, Kanpur, India
[b] Centre of Environmental Science and Engineering, CESE, IIT Kanpur, India

A B S T R A C T

A detailed time-resolved chemical characterization and volatility study of winter time ambient non refractory submicron aerosols (NR-PM_1) was conducted at Kanpur, a polluted city of India. Two very distinct, high (HL, ~ 240 μg/m^3) and low (LL, ~100 μg/m^3) aerosol loading periods were observed during the campaign, impacted by frequent fog events (n=17). On average, organic aerosols (OA) contributed nearly 60% of the total NR-PM_1 mass. Overall, OA volatility, (as measured by mass fraction of OA remaining after passing through a thermo denuder kept at 300 °C) decreased significantly (60%) from HL to LL period. OA volatility is anti-correlated to OA loading but much more strongly so in LL compared to HL period. Volatilities of different types of OAs, as identified by positive matrix factorization (PMF) method, showed significant variations (up to 300%) from HL to LL period. This indicates that nature (like oxidation state, molecular structure, functional groups) of the OAs might have changed with variations in loading conditions. The presence of fog had little or no impact on overall OA volatility, in spite of (15–30) % enhancement in the ambinet OA oxidation ratio (O/C ratio) during fog. This study examines combined effects of OA loading and fog aqueous processing on the ambient OA volatility for the first time.

1. Introduction

Submicron ambient aerosols can have a direct or indirect influence on climate forcing and adverse effects on human health (Jacobson, Hansson, Noone, & Charlson, 2000; Jimenez et al., 2009; Seinfeld & Pankow, 2003). Organic aerosols (OA) usually contributes bulk of the submicron aerosol mass (Hallquist et al., 2009; Jacobson et al., 2000; Jimenez et al., 2009) and vary greatly in terms of their sources, properties (Jacobson et al., 2000; Shamjad et al., 2015; Stackelberg, Buonocore, Bhave, & Schwartz, 2013). Several studies have reported very high aerosol loadings in all the major Indian cities including Kanpur, based on 4–12 h long filter based measurements (Gurjar, van Aardenne, Lelieveld, & Mohan, 2004; Joseph, Unnikrishnan & Kumar, 2012; Mishra & Tripathi, 2008; Sarkar, Khillare, Jyethi, Hasan, & Parween, 2010; Singh, Lakshay, & Gupta, 2014). Although useful, these offline studies provided no or little information regarding different types, sources and evolution of OA (alterations in OA composition and properties through oxidation, mixing and volatilization (Heald et al., 2010)).

Recent emergence of Aerodyne aerosol mass spectrometer (Canagaratna et al., 2007; DeCarlo et al., 2006) have offered some unique insights into ambient OA composition and evolution (Hallquist et al., 2009; Heald et al., 2010) on real time basis. Recent studies indicate that most of the current global models under- predict both total OA and secondary organic aerosols (SOA) burden in

* Corresponding authors at: Department of Civil Engineering Indian Institute of Technology, Kanpur.
E-mail addresses: snt@iitk.ac.in (S.N. Tripathi), tarun@iitk.ac.in (T. Gupta).

http://dx.doi.org/10.1016/j.jaerosci.2016.11.015
Received 22 January 2016; Received in revised form 8 August 2016; Accepted 29 November 2016
Available online 30 November 2016
0021-8502/

the atmosphere (Heald et al., 2011). This indicates that global models either include some invalid assumptions and/or missing some key processes/factors that control the fate of ambient OA. 'Volatility' of OA is one of those factors, which describes affinity of different types of OA towards particle or gas phase. Atmospheric reactivity and removal rate of different types of OA, like freshly emitted primary OA and freshly oxidized SOA, depend on their respective volatilities (Bidleman, 1988). Volatility studies are mostly conducted using a thermodenuder (TD). TD consists of heating and denuding sections; a heated hollow metal tube wrapped with heating coils (heating part) followed by a cooling section with absorbents (mostly charcoal) (denuder part). TD removes volatile species from the aerosols by first heating the aerosols at a particular temperature and then absorbing the volatiles into the absorbent.

Many ambient and smog chamber studies have already reported volatilities of ambient and laboratory generated SOA (mostly from gas phase oxidation of known volatile organic precursors) by combining a TD with an Aerodyne AMS (Huffman et al., 2009; Kang, Toohey, & Brune, 2011; Pfaffenberger et al., 2013; Poulain et al., 2014). Kang et al., (2011) from a laboratory study found that SOA volatility decreases with increasing oxidation ratio (O/C) and decreasing OA loading, but the rate of decrease depends on OA loading regime. Huffman et al. (2009) from an ambient study reported that almost all types of OAs are somewhat semi volatile in nature. Both Huffman et al. (2009) and Poulain et al. (2014) found that at higher temperatures most of the aerosol mass fraction remaining (MFR, a proxy for volatility) was organics, indicating that a portion of ambient OA is of non-volatile in nature.

Few laboratory studies have also reported volatility information of SOA formed via aqueous phase oxidation (AqSOA) (Ortiz-Montalvo et al., 2014; Ortiz-Montalvo, Lim, Perri, Seitzinger, & Turpin, 2012; Sorooshian, Wang, Coggon, Jonsson, & Ervens, 2013; Yu et al., 2014). AqSOA is usually comprised of more oxidized, hygroscopic organic compounds like organic acids and expected to be less volatile than gaseous SOA (Ervens, Turpin, & Weber, 2011). However, studies on the volatility of ambient aqSOA formed in clouds, fogs and wet aerosols are very rare. Since aqSOA is a significant part of total SOA (Ervens et al., 2011), it is important to study its impact on the overall OA volatility. The objective of this study was to explore the dependence of OA volatility on different aerosol loading regime and foggy conditions (favorable for the production of aqSOA) at a polluted urban site.

2. Materials and methods

2.1. Measurement site and study period

Measurement was carried out at Indian Institute of Technology (IIT) Kanpur, India (26.5 °N, 80.3 °E, and 142 m above MSL). Kanpur is a sprawling urban center with a population of ≃4.5 million (Chakraborty, Bhattu, Gupta, Tripathi, & Canagaratna, 2015; GOI, 2011), located at the heart of the Gangetic Plain (GP) but has poor air quality (Chakraborty et al., 2015; National ambient air quality standards, 2012). Based on ambient NR-PM_1 loading the entire measurement period was split into two separate periods: the 1st period termed as high loading (HL) period spanning from 18 Dec, 2014-01 Jan, 2015 with an average NR-PM_1 loading of 239 (± 73) μg/m^3 and numerous frequent fog events (10 events in 15 days). The 2nd period is termed as low loading (LL) period spanning from 02 Jan 2015 – 10 February, 2015 with an average NR-PM_1 loading of 101 (± 39) μg/m^3, and several infrequent fog events (7 events in 40 days). Meteorological and emission parameters for both the periods are listed in Table 1. RH & T values were obtained from Vaisala RH & T sensor (Model: HMT 331), deployed at the same laboratory along with other instruments. Wind speed (DWA 8600, Dynalab Weathertech), precipitation (DTR 8104, Dynalab Weathertech), and solar radiation (CMP 6, Kripp & Zonen) data were obtained from an automated weather station located near vicinity while the PBL heights were obtained from NOAA ARL archive. CO data was obtained from Thermo Fisher CO analyzer (Model: 49i) instrument kept at the rooftop of the laboratory building.

In order to analyze the effects of fog on aerosol volatility, we further divided both the HL and LL period into several sub periods like pre foggy/non pre foggy (PrF/NPrF), foggy/non foggy night (Fog/NFN), post foggy/non post foggy periods (PoF/NPoF). Pre foggy (PrF) period is 5 h time span before the commencement of a fog event while post foggy (PoF) period is daytime hours (till 6 pm) after fog dissipation. Fog hours were mostly observed between 11pm–8am (Fog), so pre fog (PrF) period is 6–11 pm and post fog period (PoF) is 8am–6pm. Identical time periods are taken for non foggy periods, and termed as non foggy night (NFN), non pre foggy (NPrF), and non post foggy period (NPoF). Fog is usually defined in terms of visibility [visibility < 1 km and RH is close to 100%].

Table 1
Average (± 1 std) values for different meteorological and emission parameters during HL and LL period. PBL = Boundary layer height, WS = Wind speed, SR = Solar radiation, CO = Carbon monoxide.

Parameters	HL			LL		
	Non fog		Fog	Non fog		Fog
	Day	Night		Day	Night	
RH (%)	74.25 ± 8.2	87.43 ± 5.1	96.9 ± 2.9	73.84 ± 6.8	86.79 ± 6.8	95.8 ± 3.5
T (°C)	12.93 ± 3.8	9.82 ± 2.6	7.24 ± 2.1	14.24 ± 3.9	11.15 ± 2.2	7.53 ± 1.9
PBL (m)	492 ± 80	100 ± 28	101 ± 22	550 ± 92	141 ± 30	102 ± 25
WS (m/s)	2.95 ± 0.9	2.72 ± 0.8	1.90 ± 0.5	2.76 ± 1	2.63 ± 0.4	1.82 ± 0.6
CO (ppm)	1.16 ± 0.2	1.28 ± 0.3	1.32 ± 0.2	1.06 ± 0.3	1.13 ± 0.4	1.15 ± 0.2
SR (W/m^2)	351 ± 100			231 ± 60		
Rainfall (mm)	0			26.1		

However, for this study due to the absence of visibility measurements, the beginning of a fog event was marked when LWC (liquid water content) ≥ 80 mg/m^3 for $\geq$ 15 min (Chakraborty et al., 2015; Gilardoni et al., 2014) and end of a fog event was marked when LWC $<$ 80 mg/m^3 for $>$ 15 min (Fig. S1).

2.2. Instrumentation

A HR-ToF-AMS (high-resolution time-of-flight aerosol mass spectrometer) (Canagaratna et al., 2007; DeCarlo et al., 2006) was utilized and supported by an array of other instruments, like cloud combination probe (CCP, DMT, to measure the LWC) and E-BAM (Environment proof – Beta Attenuation Monitor, Met One Instruments, USA) for measuring $PM_{2.5}$ mass concentration at every 15 min interval. Although PM_1 inlet of AMS does not allow direct sampling of fog droplets but AMS can detect the fog processed organic residues left behind after fog evaporation. Fog processed residues are often more oxidized than interstitial aerosols as reported in several AMS based fog related field studies (Chakraborty et al., 2015; Ge, Zhang, Sun, Ruehl, & Setyan, 2012; Li, Lee, Yu, Ng, & Chan, 2013). The CCP was positioned at the rooftop of the laboratory building (at a height of 10 m above the ground) inside which other instruments were housed. The CCP can characterize a range of cloud related parameters but in this study only the CDP (cloud droplet probe) part was put to use for measurement of LWC and droplet size distributions from 3 to 50 μm (Lance, Brock, Rogers, & Gordon, 2010). AMS measurement was done via high sensitivity V mode with a 2 min averaging time, frequent problems with ToF-MS hard mirror voltage forced the discontinuation of W mode. A silica gel drier was always kept before AMS inlet to remove excessive moisture from ambient aerosols. For the AMS + TD measurements, dried ambient aerosols were switched at every 10 min and send either directly to AMS or passed through the TD kept at 300 °C to AMS. TD was built in-house with a 1 m heating section and having a 1 cm internal diameter followed by a 1 m long charcoal denuder section to prevent re-condensation of absorbed volatilized material, aerosol residence time (RT) inside the TD was 15 s. This residence time was comparable to that reported in the literature (An, Pathak, Lee, & Pandis, 2007; Huffman et al., 2009). Usually in TD studies, measurements are taken at different temperatures, but few field studies (Poulain et al., 2014; Thornberry et al., 2010) have also been carried out at a fixed temperature. As the main objective of this study is to compare OA volatilities in different loading and ambient conditions (HL vs LL, fog vs no fog), a fixed temperature served the purpose. The AMS was calibrated for inlet flow, ionization efficiency (IE), and particle sizing as per standard methods (Drewnick et al., 2005; Jayne et al., 2000; Jimenez et al., 2003). Regular IE calibrations were performed throughout the campaign. Apart from that, HEPA/zero particle (High efficiency particulate arrestance, Whatman) filter measurements were carried out on every alternate day and during IE calibrations to rectify the AMS mass spectra for gaseous interference.

2.3. Data analysis

The AMS unit-mass-resolution (UMR) and high-resolution (HR) data were analyzed in IgorPro using the data analysis toolkit SQUIRREL (v1.51 H) and PIKA (v1.10 H), respectively. HR fitting was carried out up to *m/z* 150. For both the periods, all ambient data lies well within the f44 vs. the f43 space typically defined for the ambient measurements (Ng et al., 2011). In AMS, m/z 44 or CO_2^+ fragment is considered to be a marker for carboxylic acid moieties (Takegawa et al., 2006a), and f44 is the fractional contribution of m/z 44 (f44 = m/z 44/total OA). In AMS, m/z 43 or $C_2H_3O^+$ fragment is a marker for less oxidized aldehyde or ketone moieties (Takegawa et al., 2006b), and f43 is the fractional contribution of m/z 43 (f43 = m/z43/total OA). More details regarding data-processing procedures can be found elsewhere (Aiken et al., 2008; Aiken, DeCarlo, & Jimenez, 2007; Allan, 2003). PMF analysis was carried out on HR OA spectra of entire dataset including thermally denuded part using the PMF evaluation tool (PET) (Paatero & Tapper, 1994; Ulbrich, Canagaratna, Zhang, Worsnop, & Jimenez, 2009). For ambient data set, a CE_{amb} (collection efficiency) value of 0.5 is used in this study, similar to what has been reported in other AMS studies at the same location (Bhattu & Tripathi, 2015; Chakraborty et al., 2015; Shamjad et al., 2015). The choice of this CE value was further justified by a good agreement between AMS vs E-BAM mass concentrations (Fig. S2). Other AMS measurement uncertainties are well described in the previously published literatures (Aiken et al., 2007; Allan, 2003; Bahreini et al., 2009). The standard AMS fragmentation table was modified at *m/z* values of 15, 29, and 44 respectively, utilizing HEPA filter measurements. Denuded aerosols were highly acidic due to enhanced contributions from less volatile sulfate, so CE of denuded aerosols was calculated using composition dependent formulation from Middlebrook, Bahreini, Jimenez, and Canagaratna (2012). TD studies have many uncertainties like losses inside TD, whether RT is sufficient to reach equilibrium inside TD, extent of re-condensation of volatilized organic vapors on aerosols in low temperature zones at charcoal denuder section and possibility of chemical changes occurring inside the TD (An et al., 2007; Huffman et al., 2009; Huffman, Ziemann, Jayne, Worsnop, & Jimenez, 2008; Lee et al., 2010). However, the main objective of this study is to compare OA volatility under different loading (high vs low) and ambient conditions (fog vs no fog), so our inferences are relatively immune to those uncertainties, as we maintained the same set up throughout the campaign. For both the periods air masses mostly arrived from the north-northwest as observed from back trajectory analysis, which is the predominant wind direction during this season at this location (Behera & Sharma, 2010; Chakraborty et al., 2015; Patidar, Tripathi, Bharti, & Gupta, 2012).

3. Results and discussions

3.1. Overall fog and aerosol characteristics

Campaign average fog LWC and droplet number (N_d) concentrations are 149 (± 61) mg/m^3 and 110 (± 56) cm^{-3}, respectively. These values are well within the range reported for polluted radiation fogs from around the world (Gultepe & Isaac, 1999; Gultepe

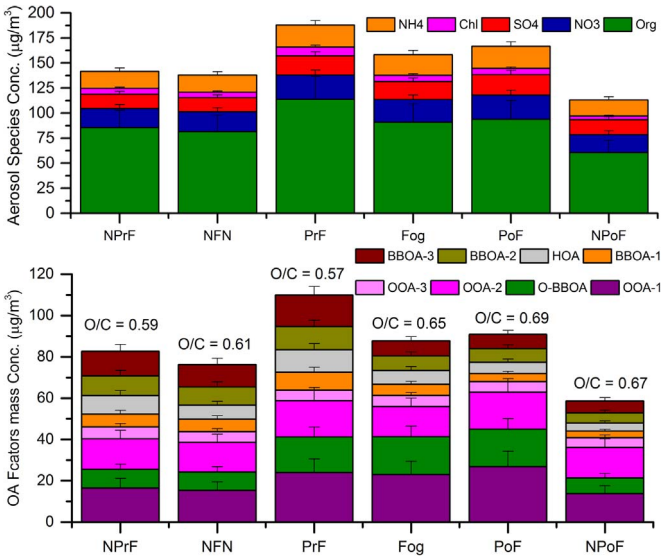

Fig. 1. Campaign average ambient NR PM_1 and OA composition before, during and after fog events. Error bars are showing only + 1 standard deviations for better clarity. NPrF = Non-pre fog, NFN = non foggy nights, PrF = Prefog, PoF = Postfog, and NPoF = Non post foggy periods, respectively.

et al., 2009; Jia-wei, Hui-wen, Zhao-ze, & Chun-sheng, 2013; Quan et al., 2011). Fog LWC and N_d values were higher for HL (170 mg/m^3 and 130 cm^{-3}, respectively) than LL (118 mg/m^3 and 80 cm^{-3}, respectively). Aerosol number concentrations (> 0.1 μm) were also much higher in HL period (7428 cm^{-3}) than LL period (5209 cm^{-3}). Aerosol and fog/cloud droplet number concentrations are usually correlated (McFarquhar et al., 2011) so less aerosol loading may have led to less dense fog during LL period compared to HL one. However, there could be several other reasons (like meteorology) for such observations but detail discussions on aerosol effects on fog microphysical properties are beyond the scope of this manuscript.

Overall, organics contributed most (82 ± 26 μg/m^3, 56%) to the observed NR PM_1 loading (143 ± 40 μg/m^3) in line with other studies at this location (Bhattu & Tripathi, 2015; Chakraborty et al., 2015; Kaul, Gupta, Tripathi, Tare, & Collett, 2011; Tare et al., 2006). Nitrate (21 ± 6 μg/m^3) and sulfate (16 ± 5 μg/m^3) were the other two major dominating species. These values were calculated using a CE value of 0.5, obtained from Middlebrook et al. (2012) formulation. NR PM_1 mass concentration is well within the range of previously reported PM_1 values (100–530 μg/m^3) at this location (Bhattu & Tripathi, 2015; Gupta & Mandariya, 2013; Kaul, Gupta, & Tripathi, 2012, 2011; Tare et al., 2006). From PrF to fog, aerosol loading decreased from 188 (± 42) μg/m^3 to 158 (± 32) μg/m^3 (Fig. 1) (difference is statistically significant, $p < 0.0001$), most likely due to fog scavenging. However, NR PM_1 composition changed little from PrF to PoF (Fig. 1), indicating that scavenging and removal were equally effective for all the species. Surprisingly, aerosol loading (158 ± 32 μg/m^3) during fog was higher than that of NFN (133 ± 38 μg/m^3) (difference is statistically significant, $p < 0.0001$) in spite of fog scavenging. This is possibly due to a combination of higher PrF aerosol loading and fog production of different secondary species (Sulfate, Nitrate, SOA) which may have negated the effect of fog scavenging and removal to some extent.

Denuded NR PM_1 aerosol mass and composition also dominated by organics (Fig. 2) followed by sulfate and nitrate. Relative contributions of denuded OA to denuded NR PM_1 (~72%) was much higher than that of ambient OA to ambient NR PM_1 (~55%, Fig. 2), indicating that least volatile materials of ambient NR PM_1 are dominated by organics. CE (collection efficiency) for denuded aerosols found to be much higher (on average, $CE_{denuded} = 0.80$) than that of ambient aerosols ($CE_{amb} = 0.50$). Particle transmission

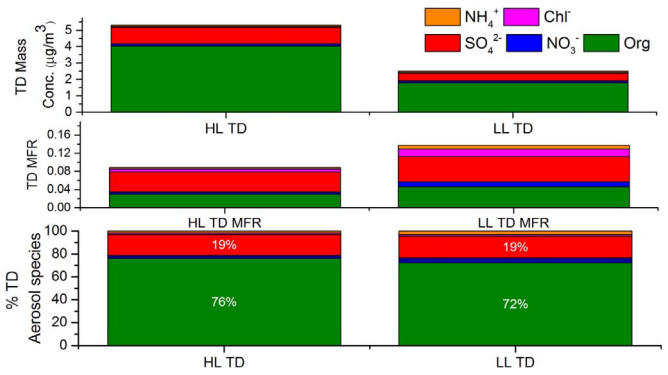

Fig. 2. Thermally denuded (TD) NR PM_1 mass concentrations, mass fraction remaining (MFR) and composition in different loading regimes.

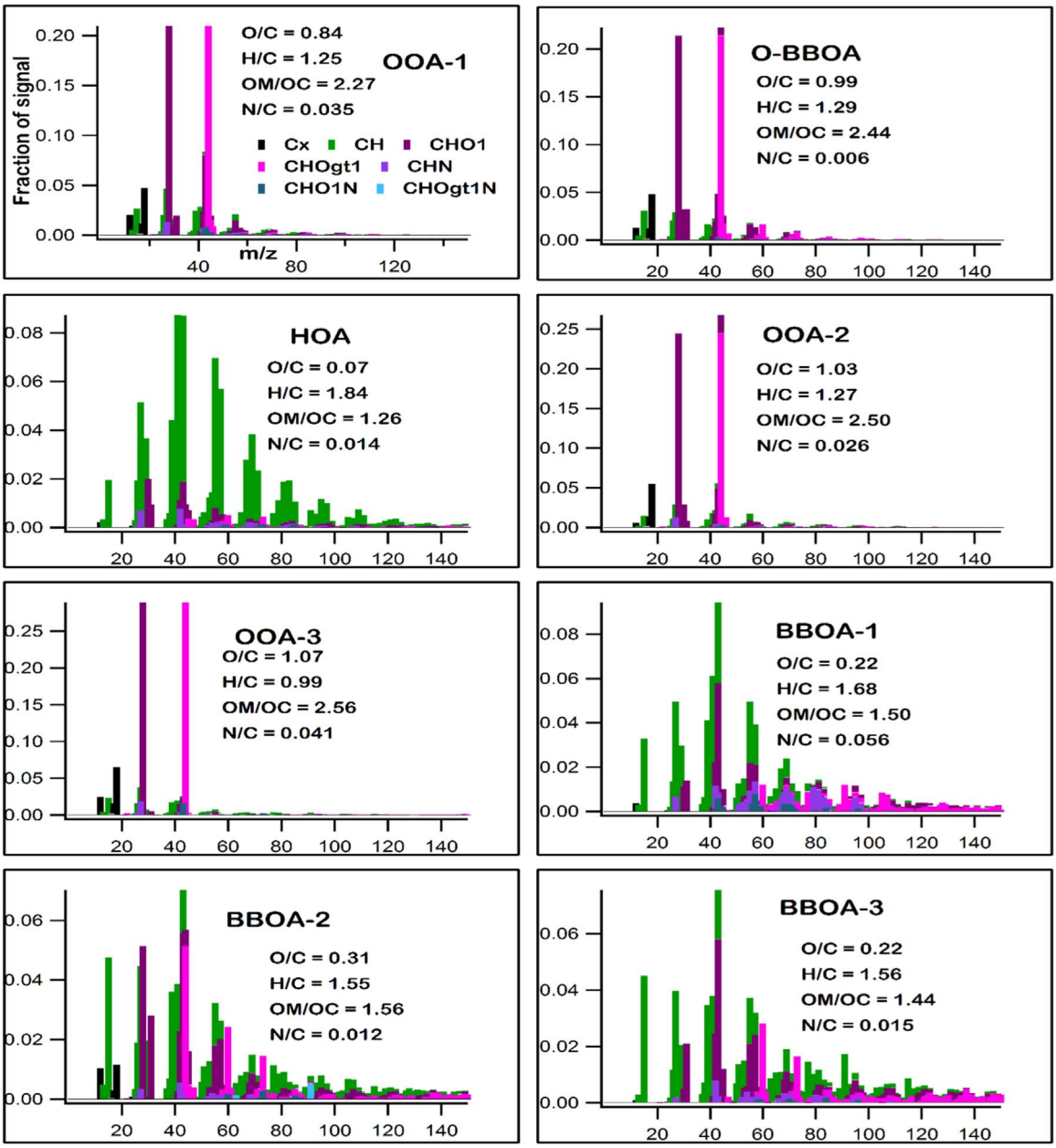

Fig. 3. Combined (TD + Ambient) HR PMF factors. OOA-1,2,3 = Different oxidized OAs. O-BBOA = Oxidized/secondary BBOA. HOA = Hydrocarbon like OA, BBOA-1,2,3 = Different primary BBOAs.

losses inside TD were characterized via ambient non-volatile black carbon measured by SP-2, on average 14% particle losses were observed inside TD (Fig. S3). So, calculated MFR (mass fraction remaining, denuded mass/ambient mass) is corrected for both CE variability from ambient to denuded aerosols and transmission losses inside TD. Being a volatile species, presence of nitrate even after heating at 300 °C is a bit surprising but has been reported before (Gkatzelis et al., 2016). We found that NO^+/NO_2^+ ratio, which is often used to verify the presence of organo nitrates (ON) (Farmer et al., 2010), increased many folds after passing through TD (=9.30) compared ambient (=3.44). This ratio (=9.30) is also 4 times higher than that of pure NH_4NO_3 (=2.30), so denuded aerosols may contain a substantial amount of ON.

Diurnal variations of different aerosol species were weak and very similar to what was reported for 2012–13 winter campaign. Night time increase of all species concentration can be attributed to lower boundary layer heights, a sharp increase in organic concentration was mostly due to enhance local biomass burning activities (Kaul et al., 2011) as evident from OA diurnal variations discussed later. ANR (aerosol neutralization ratio, is defined as ratio of NH_4^+ measured by AMS to NH_4^+ required to neutralize anions) was always close to or more than 1, indicating completely neutralized ambient aerosols and presence of excess ammonium.

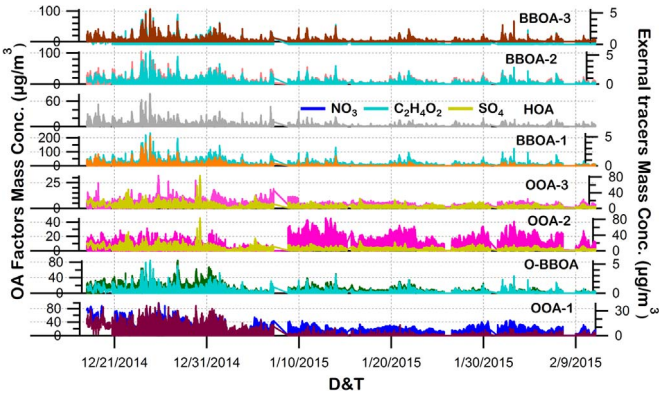

Fig. 4. Combined (TD + Amb) HR PMF OA Factors vs tracers.

On the contrary, denuded aerosols were highly acidic due to dominance of non-volatile sulfate as also reported in many previous TD + AMS studies (Huffman et al., 2009; Poulain et al., 2014).

3.2. Composition

Source apportionment of OA via PMF revealed 4 oxidized (or secondary) and 4 primary OA factors including one aged/oxidized biomass burning OA (O-BBOA) (Fig. 3). For PMF diagnostics, the rationale behind choosing 8 factor solution, ambient and TD OA composition and OA diurnal variations please refer to Supplementary information (SI,Table S1 and Fig. S4-S8). Chosen PMF factors correlation with external tracers (apart from BBOA factors for which m/z 60 is used due to lack of external tracers) and PMF diagnostics are shown in Fig. 4. OOA factors correlate well with Nitrate and Sulfate confirming their secondary nature and different volatilities. In brief, during HL period OA mass concentration and O/C were 134 ± 42 μg/m^3 and 0.59 ± 0.09, respectively. During LL period OA mass concentration and O/C were 56 ± 20 μg/m^3 and 0.69 ± 0.1, respectively (for both the parameters, HL and LL periods differences are very statistically significant, $p < 0.0001$). These differences in mass concentrations were most likely caused by lower anthropogenic emissions (as indicated by lower CO values in Table 1) combined with higher daytime boundary layer heights and sporadic light rainfall (Table 1) during LL period. Fog impact on OA characteristics can be clearly seen from Fig. 1, where O/C ratio increased significantly from prefog (=0.57) to fog period (=0.65), but remained unchanged from NPrF to NFN period. Total OOA (OOA-1,2,3 + O-BBOA) contributions to OA also increased significantly from prefog (57%) to fog (70%) but remained almost unchanged from NPrF (56%) to NFN (58%). Total OOA mass concentration and relative contributions are also much higher during foggy period (61 μg/m^3 & 70%) compared to NFN (43 μg/m^3 & 58%), in spite of scavenging. PoF period also has higher mass concentration and relative contributions (68 μg/m^3 & 75%) from total OOA compared to NPoF period (42 μg/m^3 & 68%) (Fig. 1). A previous study (Chakraborty, Ervens, Gupta, & Tripathi, 2016) on characterization of fog droplet residues at this location have already shown the enhanced aqueous processing of existing OA inside the fog droplets and the formation of highly oxidized OA. Fig. S5 also shows that fog impacted both HL and LL period OA characteristics and composition significantly. These changes clearly indicate that fog can influence OA characteristics and composition significantly via aqueous processing and scavenging.

3.3. Impact of OA loading on OA volatility

Ambient OA volatility is found to be positively correlated (or MFR is negatively correlated) with ambient OA loading but intensity of the correlation is loading regime dependent (Fig. 5). In LL condition the slope of this correlation is much steeper than during HL condition. A similar finding was reported by Kang et al. (2011) from smog chamber study conducted on α-pinene although such relationship has rarely been reported from field studies. Negative impact of OA loading on MFR can be explained by the observed

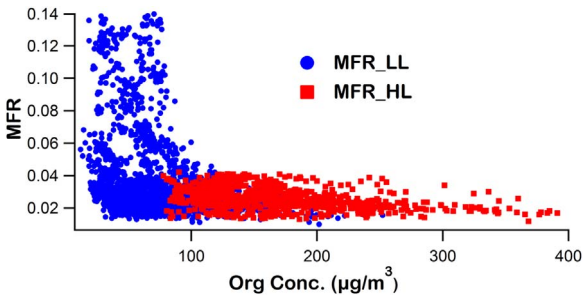

Fig. 5. Decreasing OA MFR (mass fraction remaining) or increasing OA volatility with increasing OA concentrations.

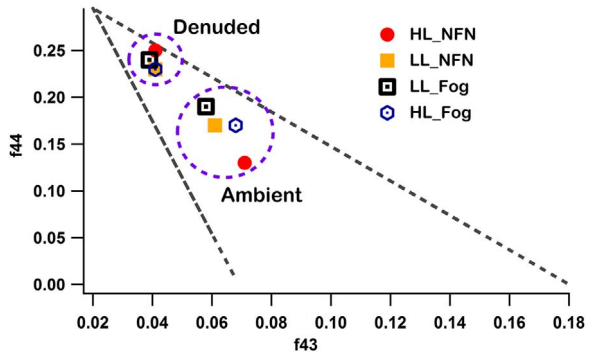

Fig. 6. Triangle plot (f44 vs f43) for ambient and thermally denuded OAs. Dashed line indicate the region within which most of the ambient data generally resides (Ng et al., 2011). Differences in f44 and f43 levels of ambient OA in different periods (lower circle) diminished after heating at 300 °C (upper circle).

anti-correlation between O/C and OA loading (Fig. S9). Usually OA volatility decreases (MFR increases) with increasing oxidation (Huffman et al., 2009; Jimenez et al., 2009; Yu et al., 2014). On the contrary with increasing OA loading, partitioning of less oxidized OA into particle phase increases as indicated by enhanced $C_2H_3O^+$ (Fig. S10) fraction. Contributions of relatively more volatile POAs also increased with the loading (discussed later). Therefore increasing OA loading and decreasing O/C ratio cause a decline in MFR during HL period. So, HL OA MFR value (0.029 ± 0.006) is expectedly lower than LL OA (0.045 ± 0.01) (difference is statistically very significant, $p < 0.0001$). Similar low OA MFR values have been reported from other ambient TD studies carried out at high temperatures like 300 °C or 400 °C (Gkatzelis et al., 2016; Poulain et al., 2014; Thornberry et al., 2010). However, volatility and O/C correlation is not universal as several other parameters like carbon number, molecular structures, ambient conditions (Donahue, Robinson, Trump, Riipinen, & Kroll, 2014; Kroll et al., 2011; Paciga et al., 2016; Tritscher et al., 2011) can also influence OA volatility. So, the possible role of other such factors in observed anti-correlation between OA loading and MFR cannot be ruled out completely.

In Fig. 5, f44 levels of the denuded OAs (points inside the upper circle of Fig. 6) are almost the same under different conditions in spite of marked differences in their ambinet levels (lower circle of Fig. 6). This also indicates that O/C ratio (directly correlated to f44) of denuded, low volatile OA remained almost constant throughout the campaign. Therefore, observed ambient O/C ratio changes occurred due to condensation of semi to moderately volatile organics on to this low volatile OA, EC (elemental carbon), BC (black carbon). Like in ambient NR-PM_1, OA remained the most dominant species in the denuded NR PM_1 mass (Fig. 2). Interestingly, apart from OA, MFR values of inorganics like Sulfate, Chloride and Nitrate increased substantially (Fig. 2) from HL to LL period. The exact reason for this is not clear to us but may be mixing with different types of organics under different loading conditions may have affected inorganics volatility (Häkkinen, McNeill, & Riipinen, 2014).

The steeper decrease of O/C ratio under LL condition can be explained by the rapid decline in relative contribution of OOA-2 (dominant OOA during LL period) with loading (0.16% reduction per μg m^{-3} of OA loading increase) (Fig. S11). In comparison, OOA-1 (dominant OOA during HL period); decreases moderately with loading (0.04% reduction per μg m^{-3} increase in OA loading,. Also, OOA-2 has much higher O/C (=1.03) than OOA-1 (=0.84) (Fig. 3), so a rapid decrease of OOA-2 during LL period has made rate of O/C ratio decline even higher with increasing OA loading.

Fig. 7 demonstrated that OOA-3 is the least volatile OA component but during LL period with increasing OA loading its relative contribution decreases much rapidly (11% to 2%) compared to HL period (7% to 4%) (Fig. S11). This has also contributed to relatively steeper decrease in MFR with increasing OA loading during LL period than HL period. Overall MFR of OOA-2 (0.016 ±

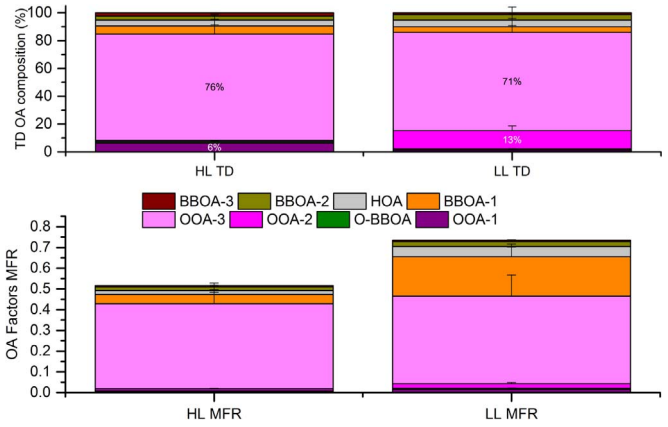

Fig. 7. MFR of different OA factors under different total OA loading conditions. Error bars are showing on +1 standard deviation for better clarity.

0.005) is higher than OOA-1 (0.01 ± 0.004) (difference is statistically very significant, $p < 0.0001$), indicating OOA-2 is relatively more non-volatile than OOA-1 (Fig. 7), in line with their O/C ratios. Fig. 7 also shows that the influence of OA loading regime on volatilities vary greatly for different types of OAs. Most significant changes (increase) in MFR (and decrease in volatility) are observed in BBOA-1 (5 fold), HOA (3 fold), while OOA-3 MFR remained unchanged from HL to LL period. This indicates that nature (like oxidation state, molecular structure, functional groups, etc.) of some of the OAs might have changed with variations in loading conditions. Similar finding has also been reported by Poulain et al. (2014) and possible changes in OA oxidation state and/or origins are listed as probable cause of such observation. It is also interesting to note that O-BBOA has much lower MFR values compared to primary BBOAs (BBOA-1,2,3), in spite of being more oxidized than them. So, O/C and volatility relationship is very complex and not always (anti)correlates with each other.

Volatility of different OA functional groups also seemed to vary with OA loading (Fig. S12), with biggest changes occurring in less oxidized CHO1 functional groups (decrease) and CHOgt1N (organo nitrates) functional groups (increase). This observation signifies that some fragments belonging to these broad functional groups possibly came from different parent organic compounds during different loading periods.

On an individual basis, CO_2^+ fragment (a tracer for highly oxidized OA) is much less volatile than $C_2H_3O^+$ (a tracer of less oxidized OA) however, on an overall basis, CHOgt1 functional group, with higher oxygen content has higher volatility than CHO1 group (Fig. S12). This observation can be explained by the presence of highly volatile fragments like $C_2H_4O_2^+$ (Huffman et al., 2009), in CHOgt1 functional group. Such highly volatile groups are contributing to the observed higher volatility of CHOgt1 functional group compared to CHO1 group.

3.4. Effects of fog on OA volatility

Fog (aqueous) processing can produce aqSOA (aqueous SOA) (Ervens et al., 2011; Ge et al., 2012; Kaul et al., 2011), which are usually more oxidized and less volatile than SOA produced from gas-phase reactions (Ervens et al., 2011) as reported from some previous lab studies (Yu et al., 2014). Nevertheless, impact of fog on OA volatility under ambient conditions has never been studied. Since ambient conditions are much more complex than ideal lab conditions, in terms of different types of precursors, meteorological conditions etc. therefore it is important to understand the actual impact of fog (aqueous) processing on overall ambient OA volatility. From prefog to foggy period, OA loading showed a decrease(from 137 ± 50 μg/m^3 to 109 ± 40 μg/m^3) and ambient f44 and O/C values are enhanced (Fig. 6 and S5). However, fog impact on overall OA volatility is found to be either negligible or negative during both the loading periods. During fog, for both the loading periods, the decrease in MFR was particularly pronounced for OOA-3, and to some extent for BBOA-1. For other OOAs (OOA-1,2 + O-BBOA) and POAs (HOA + BBOA-2,3), presence of fog had no or negligible impact (Fig. 8) on their volatilities.

Many previous laboratory studies reported formation of highly oxidized and low volatile diacids, oligomers via aqueous processing (Ortiz-Montalvo et al., 2014, 2012; Yu et al., 2014). These residues can remain in the particulate phase even after droplet evaporation (Limbeck, Kulmala, & Puxbaum, 2003; Ortiz-Montalvo et al., 2014, 2012). In this study, during fog, enhancement in particulate phase organic acids is indicated by enhanced f44 levels (a marker of organic acids, (Ng et al., 2011; Zhang, Jimenez, Worsnop, & Canagaratna, 2007)) (Fig. 6). Apart from that O/C ratio also increased during fog events indicating the presence of fog processed oxidized residues (Fig. 1 and S5). A detailed study (Chakraborty et al., 2016) on fog water characteristics carried out at the same location has already shown that fog droplet processed residues are indeed less volatile and will remain in particulate phase even after droplet evaporation. However, Fog and PoF OA MFR at 300 °C are either lower or comparable with other time periods (NFN/PrF/NPoF, Fig. 8), indicating that overall ambient OA volatility has not decreased in spite of increased O/C ratio and contribution from fog processed residues. A similar TD + AMS study carried out during 2013-14 winter at the same location (manuscript under preparation) but at much lower TD temperatures (100 °C and 150 °C), also showed that OA volatility varied little from foggy and non foggy periods (Fig. S13). No changes in OA volatility from nonfoggy to foggy period even at these lower TD temperatures also make it

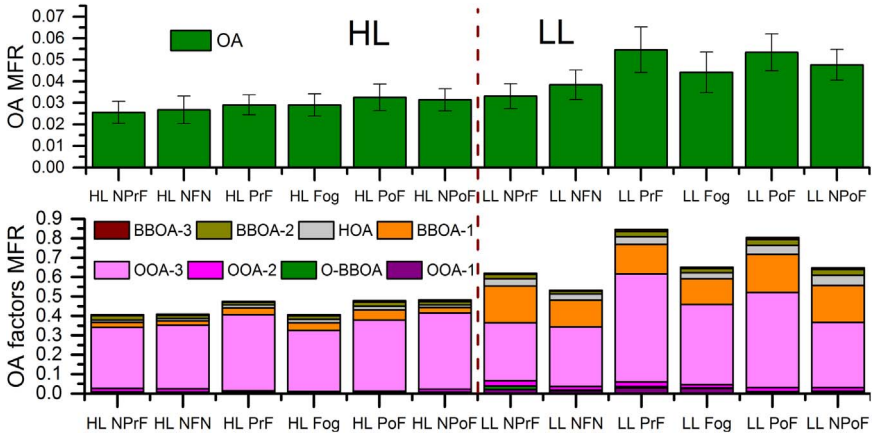

Fig. 8. Combined effects of fog and OA loading regime on different OA volatilities (mass fraction remaining, MFR). Error bars are showing ± 1 standard deviation.

unlikely that observed results at 300 °C are being affected by artifacts like formation /dissociations of oligomers inside the TD.

Although exact causes are difficult to pin point but a few possibilities can be considered to explain the similar volatility profiles of foggy and non foggy period OA with different O/C ratios. In both the loading conditions, during fog, O-BBOA contribution to total OA has increased compared to non foggy periods (Fig. S5) and in previous section, it has already been discussed that biomass burning OA are the most volatile ones (Fig. S12). Also, in ambient, low volatile aqSOA formed via fog (aqueous) processing (Chakraborty et al., 2016) are mixed with other less oxidized OAs and their volatility characteristics may have been influenced by this mixing (Tritscher et al., 2011).

4. Conclusions and atmospheric implications

Results of this study show that

1) Volatility of ambient OA is strongly correlated to existing levels of OA loading, but intensity of this correlation varies with loading regime. This observation can be explained by lower O/C ratio, variation in volatilities and contributions of different types of OAs with increasing OA loading.
2) An extremely non-volatile oxidized OA exists in this study location but its contribution to ambient OA is very less and variable [(4–10) %] under different loading regime.
3) OA fragment associated with BBOA ($C_2H_4O_2^+$) is found to be most volatile among other major fragments. However, volatility of different types of OA and organic functional groups can vary significantly with changing OA loading regime.
4) Fog has no or negative impact on ambient OA volatility in spite of enhancement in oxidation ratio (O/C ratio). Even after fog dissipation OA volatility showed no appreciable increase indicating that highly oxidized and less volatile fog processed organic residues have little impact on overall ambient OA volatility.

These results indicate that impact of aqSOA on different characteristics of existing OA under complex ambient conditions may vary significantly with some parameters are being modified positively (O/C ratio) while others (volatility) are not or negatively impacted. Presence of BBOA can make ambient OA more volatile in site of higher O/C ratios. Therefore, more field + lab studies should be conducted especially in areas impacted by biomass burning to understand how volatilities of BBOA vary with types of biomass, burning condition and oxidation. Effects of mixing of different types of OAs with different volatilities and degree of oxygenation on physicochemical properties of mixed OA should be studied in depth from lab and field studies. These studies will allow the experimentalist to obtain more meaningful results which can be of great help to the modelers for prediction of secondary organic aerosol loading and properties in actual ambient environment.

Acknowledgements

We acknowledge the support of IIT Kanpur for providing us with HR-ToF-AMS under PG research and training initiative. We would also like to acknowledge the support of Ministry of Human Resource and Development (3–21/2014-TS.1) to provide us some financial assistance to carry out this research. This research is also partially supported by through U.S. Agency for International Development (AID-OAA-A-11- 00012).

Appendix A. Supporting information

Supplementary data associated with this article can be found in the online version at doi:10.1016/j.jaerosci.2016.11.015.

References

Aiken, A. C., DeCarlo, P. F., & Jimenez, J. L. (2007). Elemental analysis of organic species with electron ionization high-resolution mass spectrometry. *Analytical Chemistry*, 79, 8350–8358. http://dx.doi.org/10.1021/ac071150w.

Aiken, A. C., Decarlo, P. F., Kroll, J. H., Worsnop, D. R., Huffman, J. A., Docherty, K. S. Jimenez, J. L. (2008). O/C and OM/OC ratios of primary, secondary, and ambient organic aerosols with high-resolution time-of-flight aerosol mass spectrometry. *Environmental Science and Technology*, 42, 4478–4485. http://dx.doi.org/10.1021/es703009q.

Allan, J. D. (2003). Correction to “Quantitative sampling using an Aerodyne aerosol mass spectrometer: 1. Techniques of data interpretation and error analysis.”. *Journal of Geophysical Research: Atmospheres*, 108. http://dx.doi.org/10.1029/2003JD001607.

An, W. J., Pathak, R. K., Lee, B.-H., & Pandis, S. N. (2007). Aerosol volatility measurement using an improved thermodenuder: Application to secondary organic aerosol. *Journal of Aerosol Science*, 38, 305–314. http://dx.doi.org/10.1016/j.jaerosci.2006.12.002.

Bahreini, R., Ervens, B., Middlebrook, A. M., Warneke, C., de Gouw, J. A., DeCarlo, P. F. Fehsenfeld, F. C. (2009). Organic aerosol formation in urban and industrial plumes near Houston and Dallas, Texas. *Journal of Geophysical Research*, 114. http://dx.doi.org/10.1029/2008jd011493.

Behera, S. N., & Sharma, M. (2010). Reconstructing primary and secondary components of PM2.5 composition for an urban atmosphere. *Aerosol Science and Technology*, 44, 983–992. http://dx.doi.org/10.1080/02786826.2010.504245.

Bhattu, D., & Tripathi, S. N. (2015). CCN closure study: Effects of aerosol chemical composition and mixing state. *Journal of Geophysical Research: Atmospheres*, 120, 766–783. http://dx.doi.org/10.1002/2014JD021978.

Bidleman, T. F. (1988). Atmospheric processes. *Environmental Science and Technology*, 22, 361–367. http://dx.doi.org/10.1021/es00169a002.

Canagaratna, M. R., Jayne, J. T., Jimenez, J. L., Allan, J. D., Alfarra, M. R., Zhang, Q. Worsnop, D. R. (2007). Chemical and microphysical characterization of ambient aerosols with the aerodyne aerosol mass spectrometer. *Mass Spectrometry Reviews*, 26, 185–222. http://dx.doi.org/10.1002/mas.20115.

Chakraborty, A., Bhattu, D., Gupta, T., Tripathi, S. N., & Canagaratna, M. R. (2015). Real-time measurements of ambient aerosols in a polluted Indian city: Sources, characteristics and processing of organic aerosols during foggy and non-foggy periods. *Journal of Geophysical Research: Atmospheres*, 120,

9006–9019. http://dx.doi.org/10.1002/2015JD023419.
Chakraborty, A., Ervens, B., Gupta, T., & Tripathi, S. N. (2016). Characterization of organic residues of size-resolved fog droplets and their atmospheric implications. *Journal of Geophysical Research: Atmospheres*, 121, 4317–4332. http://dx.doi.org/10.1002/2015JD024508.
DeCarlo, P. F., Kimmel, J. R., Trimborn, A., Northway, M. J., Jayne, J. T., Aiken, A. C. Jimenez, J. L. (2006). Field-deployable, high-resolution, time-of-flight aerosol mass spectrometer. *Analytical Chemistry*, 78, 8281–8289. http://dx.doi.org/10.1021/ac061249n.
Donahue, N. M., Robinson, A. L., Trump, E. R., Riipinen, I., & Kroll, J. H. (2014). Volatility and aging of atmospheric organic aerosol. *Topics in Current Chemisty*, 339, 97–144. http://dx.doi.org/10.1007/128-2012-355.
Drewnick, F., Hings, S. S., DeCarlo, P., Jayne, J. T., Gonin, M., Fuhrer, K. Worsnop, D. R. (2005). A new time-of-flight aerosol mass spectrometer (TOF-AMS)—instrument description and first field deployment. *Aerosol Science and Technology*, 39, 637–658. http://dx.doi.org/10.1080/02786820500182040.
Ervens, B., Turpin, B. J., & Weber, R. J. (2011). Secondary organic aerosol formation in cloud droplets and aqueous particles (aqSOA): A review of laboratory, field and model studies. *Atmospheric Chemistry and Physics*, 11, 11069–11102. http://dx.doi.org/10.5194/acp-11-11069-2011.
Farmer, D. K., Matsunaga, A., Docherty, K. S., Surratt, J. D., Seinfeld, J. H., Ziemann, P. J., & Jimenez, J. L. (2010). Response of an aerosol mass spectrometer to organonitrates and organosulfates and implications for atmospheric chemistry. *Proceedings of the National Academy of Sciences of the United States of America*, 107, 6670–6675. http://dx.doi.org/10.1073/pnas.0912340107.
Ge, X., Zhang, Q., Sun, Y., Ruehl, C. R., & Setyan, A. (2012). Effect of aqueous-phase processing on aerosol chemistry and size distributions in Fresno, California, during wintertime. *Environmental Chemistry*, 9, 221–235. http://dx.doi.org/10.1071/en11168.
Gilardoni, S., Massoli, P., Giulianelli, L., Rinaldi, M., Paglione, M., Pollini, F. Fuzzi, S. (2014). Fog scavenging of organic and inorganic aerosol in the Po Valley. *Atmospheric Chemistry and Physics*, 14, 6967–6981. http://dx.doi.org/10.5194/acp-14-6967-2014.
Gkatzelis, G. I., Papanastasiou, D. K., Florou, K., Kaltsonoudis, C., Louvaris, E., & Pandis, S. N. (2016). Measurement of nonvolatile particle number size distribution. *Atmospheric Measurement Techniques*, 9, 103–114. http://dx.doi.org/10.5194/amt-9-103-2016.
GOI (2011). Indian Census 2011, Website: 〈http://www.census2011.co.in/census/district/535-kanpur-nagar.html〉
Gultepe, I., & Isaac, G. A. (1999). Scale effects on averaging of cloud droplet and aerosol number concentrations: Observations and models. *Journal of Climate*, 12, 1268–1279. http://dx.doi.org/10.1175/1520-0442(1999)012 < 1268:SEOAOC > 2.0.CO;2.
Gultepe, I., Pearson, G., Milbrandt, J. A., Hansen, B., Platnick, S., Taylor, P. Cober, S. G. (2009). The fog remote sensing and modeling field project. *Bulletin of the American Meteorological Society*, 90, 341–359. http://dx.doi.org/10.1175/2008BAMS2354.1.
Gupta, T., & Mandariya, A. (2013). Sources of submicron aerosol during fog-dominated wintertime at Kanpur. *Environmental Science and Pollution Research*, 20, 5615–5629. http://dx.doi.org/10.1007/s11356-013-1580-6.
Gurjar, B. R., van Aardenne, J. A., Lelieveld, J., & Mohan, M. (2004). Emission estimates and trends (1990–2000) for megacity Delhi and implications. *Atmospheric Environment*, 38, 5663–5681. http://dx.doi.org/10.1016/j.atmosenv.2004.05.057.
Häkkinen, S. A. K., McNeill, V. F., & Riipinen, I. (2014). Effect of inorganic salts on the volatility of organic acids. *Environmental Science and Technology*, 48, 13718–13726. http://dx.doi.org/10.1021/es5033103.
Hallquist, M., Wenger, J. C., Baltensperger, U., Rudich, Y., Simpson, D., Claeys, M. Wildt, J. (2009). The formation, properties and impact of secondary organic aerosol: Current and emerging issues. *Atmospheric Chemistry and Physics*, 9, 5155–5236.
Heald, C. L., Coe, H., Jimenez, J. L., Weber, R. J., Bahreini, R., Middlebrook, A. M. Dunlea, E. J. (2011). Exploring the vertical profile of atmospheric organic aerosol: Comparing 17 aircraft field campaigns with a global model. *Atmospheric Chemistry and Physics*, 11, 12673–12696. http://dx.doi.org/10.5194/acp-11-12673-2011.
Heald, C. L., Kroll, J. H., Jimenez, J. L., Docherty, K. S., Decarlo, P. F., Aiken, A. C. Artaxo, P. (2010). A simplified description of the evolution of organic aerosol composition in the atmosphere. *Geophysical Research Letters*, 37. http://dx.doi.org/10.1029/2010GL042737.
Huffman, J. A., Docherty, K. S., Aiken, A. C., Cubison, M. J., Ulbrich, I. M., DeCarlo, P. F. Jimenez, J. L. (2009). Chemically-resolved aerosol volatility measurements from two megacity field studies. *Atmospheric Chemistry and Physics*, 9, 7161–7182.
Huffman, J. A., Ziemann, P. J., Jayne, J. T., Worsnop, D. R., & Jimenez, J. L. (2008). Development and characterization of a fast-stepping/scanning thermodenuder for chemically-resolved aerosol volatility measurements. *Aerosol Science and Technology*, 42, 395–407. http://dx.doi.org/10.1080/02786820802104981.
Jacobson, M. C., Hansson, H. C., Noone, K. J., & Charlson, R. J. (2000). Organic atmospheric aerosols: Review and state of the science. *Reviews of Geophysics*, 38, 267–294. http://dx.doi.org/10.1029/1998rg000045.
Jayne, J. T., Leard, D. C., Zhang, X. F., Davidovits, P., Smith, K. A., Kolb, C. E., & Worsnop, D. R. (2000). Development of an aerosol mass spectrometer for size and composition analysis of submicron particles. *Aerosol Science and Technology*, 33, 49–70. http://dx.doi.org/10.1080/027868200410840.
Jia-wei, Z., Hui-wen, X. U. E., Zhao-ze, D., & Chun-sheng, Z. (2013). Effects of aerosols on fogs observed in the North China plain. *Atmospheric Oceanic Science Letters*, 6, 79–83. http://dx.doi.org/10.1080/16742834.2013.11447060.
Jimenez, J. L., Canagaratna, M. R., Donahue, N. M., Prevot, A. S. H., Zhang, Q., Kroll, J. H. Worsnop, D. R. (2009). Evolution of organic aerosols in the atmosphere. *Science*, 326, 1525–1529. http://dx.doi.org/10.1126/science.1180353.
Jimenez, J. L., Jayne, J. T., Shi, Q., Kolb, C. E., Worsnop, D. R., Yourshaw, I. Davidovits, P. (2003). Ambient aerosol sampling using the aerodyne aerosol mass spectrometer. *Journal of Geophysical Research*, 108. http://dx.doi.org/10.1029/2001jd001213.
Joseph, A. E., Unnikrishnan, S., & Kumar, R. (2012). Chemical characterization and mass closure of fine aerosol for different land use patterns in Mumbai city. *Aerosol and Air Quality Research*, 12, 61–72. http://dx.doi.org/10.4209/aaqr.2011.04.0049.
Kang, E., Toohey, D. W., & Brune, W. H. (2011). Dependence of SOA oxidation on organic aerosol mass concentration and OH exposure: Experimental PAM chamber studies. *Atmospheric Chemistry and Physics*, 11, 1837–1852. http://dx.doi.org/10.5194/acp-11-1837-2011.
Kaul, D. S., Gupta, T., & Tripathi, S. N. (2012). Chemical and microphysical properties of the aerosol during foggy and nonfoggy episodes: A relationship between organic and inorganic content of the aerosol. *Atmospheric Chemistry Physics Discussion*, 12, 14483–14524. http://dx.doi.org/10.5194/acpd-12-14483-2012.
Kaul, D. S., Gupta, T., Tripathi, S. N., Tare, V., & Collett, J. L., Jr. (2011). Secondary organic aerosol: A comparison between foggy and nonfoggy days. *Environmental Science and Technology*, 45, 7307–7313. http://dx.doi.org/10.1021/es201081d.
Kroll, J. H., Donahue, N. M., Jimenez, J. L., Kessler, S. H., Canagaratna, M. R., Wilson, K. R. Worsnop, D. R. (2011). Carbon oxidation state as a metric for describing the chemistry of atmospheric organic aerosol. *Nature Chemistry*, 3, 133–139. http://dx.doi.org/10.1038/nchem.948.
Lance, S., Brock, C. a, Rogers, D., & Gordon, J. a (2010). Water droplet calibration of the Cloud Droplet Probe (CDP) and in-flight performance in liquid, ice and mixed-phase clouds during ARCPAC. *Atmospheric Measurement Techniques*, 3, 1683–1706. http://dx.doi.org/10.5194/amt-3-1683-2010.
Lee, B. H., Kostenidou, E., Hildebrandt, L., Riipinen, I., Engelhart, G. J., Mohr, C. Pandis, S. N. (2010). Measurement of the ambient organic aerosol volatility distribution: Application during the Finokalia Aerosol Measurement Experiment (FAME-2008). *Atmospheric Chemistry and Physics*, 10, 12149–12160. http://dx.doi.org/10.5194/acp-10-12149-2010.
Li, Y. J., Lee, B. Y. L., Yu, J. Z., Ng, N. L., & Chan, C. K. (2013). Evaluating the degree of oxygenation of organic aerosol during foggy and hazy days in Hong Kong using high-resolution time-of-flight aerosol mass spectrometry (HR-ToF-AMS). *Atmospheric Chemistry and Physics*, 13, 8739–8753. http://dx.doi.org/10.5194/acp-13-8739-2013.
Limbeck, A., Kulmala, M., & Puxbaum, H. (2003). Secondary organic aerosol formation in the atmosphere via heterogeneous reaction of gaseous isoprene on acidic particles. *Geophysical Research Letters*, 30, 4–7. http://dx.doi.org/10.1029/2003GL017738.
McFarquhar, G. M., Ghan, S., Verlinde, J., Korolev, A., Strapp, J. W., Schmid, B. Glen, A. (2011). Indirect and semi-direct aerosol campaign: The impact of arctic aerosols on clouds. *Bulletien of American Meteorological Society*, 92, 183. http://dx.doi.org/10.1175/2010bams2935.1.
Middlebrook, A. M., Bahreini, R., Jimenez, J. L., & Canagaratna, M. R. (2012). Evaluation of composition-dependent collection efficiencies for the aerodyne aerosol mass spectrometer using field data. *Aerosol Science and Technology*, 46, 258–271. http://dx.doi.org/10.1080/02786826.2011.620041.
Mishra, S. K., & Tripathi, S. N. (2008). Modeling optical properties of mineral dust over the Indian Desert. *Journal of Geophysical Research Atmospheres*, 113(1–19), D23201. http://dx.doi.org/10.1029/2008JD010048.
National ambient air quality standards (2012). *National ambient air quality status & trends in india-2010 central pollution control board*. GOI.
Ng, N. L., Canagaratna, M. R., Jimenez, J. L., Chhabra, P. S., Seinfeld, J. H., & Worsnop, D. R. (2011). Changes in organic aerosol composition with aging inferred from aerosol mass spectra. *Atmospheric Chemistry and Physics*, 11, 6465–6474. http://dx.doi.org/10.5194/acp-11-6465-2011.

Ortiz-Montalvo, D. L., Hakkinen, S. A. K., Schwier, A. N., Lim, Y. B., McNeill, V. F., & Turpin, B. J. (2014). Ammonium addition (and aerosol ph) has a dramatic impact on the volatility and yield of glyoxal secondary organic aerosol. *Environmental Science and Technology*, 48, 255–262. http://dx.doi.org/10.1021/es4035667.

Ortiz-Montalvo, D. L., Lim, Y. B., Perri, M. J., Seitzinger, S. P., & Turpin, B. J. (2012). Volatility and yield of Glycolaldehyde SOA formed through aqueous photochemistry and droplet evaporation. *Aerosol Science and Technology*, 46, 1002–1014. http://dx.doi.org/10.1080/02786826.2012.686676.

Paatero, P., & Tapper, U. (1994). Positive matrix factorization - a nonnegative factor model with optimal utilization of error estimates of data values. *Environmetrics*, 5, 111–126. http://dx.doi.org/10.1002/env.3170050203.

Paciga, A., Karnezi, E., Kostenidou, E., Hildebrandt, L., Psichoudaki, M., Engelhart, G. J. Pandis, S. N. (2016). Volatility of organic aerosol and its components in the megacity of Paris. *Atmospheric Chemistry and Physics*, 16, 2013–2023. http://dx.doi.org/10.5194/acp-16-2013-2016.

Patidar, V., Tripathi, S. N., Bharti, P. K., & Gupta, T. (2012). First surface measurement of cloud condensation nuclei over Kanpur, IGP: Role of long range transport. *Aerosol Science and Technology*, 46, 973–982. http://dx.doi.org/10.1080/02786826.2012.685113.

Pfaffenberger, L., Barmet, P., Slowik, J. G., Praplan, a P., Dommen, J., Prévôt, a S. H., & Baltensperger, U. (2013). The link between organic aerosol mass loading and degree of oxygenation: An α-pinene photooxidation study. *Atmospheric Chemistry and Physics*, 13, 6493–6506. http://dx.doi.org/10.5194/acp-13-6493-2013.

Poulain, L., Birmili, W., Canonaco, F., Crippa, M., Wu, Z. J., Nordmann, S. Herrmann, H. (2014). Chemical mass balance of 300 °C non-volatile particles at the tropospheric research site Melpitz, Germany. *Atmospheric Chemistry and Physics*, 14, 10145–10162. http://dx.doi.org/10.5194/acp-14-10145-2014.

Quan, J., Zhang, Q., He, H., Liu, J., Huang, M., & Jin, H. (2011). Analysis of the formation of fog and haze in North China Plain (NCP). *Atmospheric Chemistry and Physics*, 11, 8205–8214. http://dx.doi.org/10.5194/acp-11-8205-2011.

Sarkar, S., Khillare, P. S., Jyethi, D. S., Hasan, A., & Parween, M. (2010). Chemical speciation of respirable suspended particulate matter during a major firework festival in India. *Journal of Hazard Materials*, 184, 321–330. http://dx.doi.org/10.1016/j.jhazmat.2010.08.039.

Seinfeld, J. H., & Pankow, J. F. (2003). Organic atmospheric particulate material. *Annual Review of Physical Chemistry*, 54, 121–140. http://dx.doi.org/10.1146/annurev.physchem.54.011002.103756.

Shamjad, P. M., Tripathi, S. N., Pathak, R., Hallquist, M., Arola, A., & Bergin, M. H. (2015). Contribution of brown carbon to direct radiative forcing over the Indo-Gangetic plain. *Environmental Science and Technology*, 49, 10474–10481. http://dx.doi.org/10.1021/acs.est.5b03368.

Singh, D. K., Lakshay, & Gupta, T. (2014). Field performance evaluation during fog-dominated wintertime of a newly developed denuder-equipped PM1 sampler. *Environmental Science and Pollution Research*, 21, 4551–4564. http://dx.doi.org/10.1007/s11356-013-2371-9.

Sorooshian, A., Wang, Z., Coggon, M. M., Jonsson, H. H., & Ervens, B. (2013). Observations of sharp oxalate reductions in stratocumulus clouds at variable altitudes: Organic acid and metal measurements during the 2011 E-PEACE campaign. *Environmental Science and Technology*, 47, 7747–7756. http://dx.doi.org/10.1021/es4012383.

Stackelberg, K. V., Buonocore, J., Bhave, P. V., & Schwartz, J. A. (2013). Public health impacts of secondary particulate formation from aromatic hydrocarbons in gasoline. *Environmental Health*, 12, 1–13. http://dx.doi.org/10.1186/1476-069x-12-19.

Takegawa, N., Miyakawa, T., Kondo, Y., Blake, D. R., Kanaya, Y., Koike, M. Takeuchi, T. (2006). Evolution of submicron organic aerosol in polluted air exported from Tokyo. *Geophysical Research Letters*, 33. http://dx.doi.org/10.1029/2006gl025815.

Takegawa, N., Miyakawa, T., Kondo, Y., Jimenez, J. L., Zhang, Q., Worsnop, D. R., & Fukuda, M. (2006). Seasonal and diurnal variations of submicron organic aerosol in Tokyo observed using the Aerodyne aerosol mass spectrometer. *Journal of Geophysical Research*, 111. http://dx.doi.org/10.1029/2005jd006515.

Tare, V., Tripathi, S. N., Chinnam, N., Srivastava, A. K., Dey, S., Manar, M. Sharma, M. (2006). Measurements of atmospheric parameters during Indian Space Research Organization Geosphere Biosphere Program Land Campaign II at a typical location in the Ganga Basin: 2. Chemical properties. *Journal of Geophysical Research*, 111, D23210. http://dx.doi.org/10.1029/2006JD007279.

Thornberry, T., Froyd, K. D., Murphy, D. M., Thomson, D. S., Anderson, B. E., Thornhill, K. L., & Winstead, E. L. (2010). Persistence of organic carbon in heated aerosol residuals measured during Tropical Composition Cloud and Climate Coupling (TC4). *Journal of Geophysical Research Atmospheres*, 115(1–10), D00J02. http://dx.doi.org/10.1029/2009JD012721.

Tritscher, T., Dommen, J., DeCarlo, P. F., Gysel, M., Barmet, P. B., Praplan, A. P. Baltensperger, U. (2011). Volatility and hygroscopicity of aging secondary organic aerosol in a smog chamber. *Atmospheric Chemistry and Physics*, 11, 11477–11496. http://dx.doi.org/10.5194/acp-11-11477-2011.

Ulbrich, I. M., Canagaratna, M. R., Zhang, Q., Worsnop, D. R., & Jimenez, J. L. (2009). Interpretation of organic components from positive matrix factorization of aerosol mass spectrometric data. *Atmospheric Chemistry and Physics*, 9, 2891–2918.

Yu, L., Smith, J., Laskin, A., Anastasio, C., Laskin, J., & Zhang, Q. (2014). Chemical characterization of SOA formed from aqueous-phase reactions of phenols with the triplet excited state of carbonyl and hydroxyl radical. *Atmospheric Chemistry and Physics*, 14, 13801–13816. http://dx.doi.org/10.5194/acp-14-13801-2014.

Zhang, Q., Jimenez, J. L., Worsnop, D. R., & Canagaratna, M. (2007). A case study of urban particle acidity and its influence on secondary organic aerosol. *Environmental Science and Technology*, 41, 3213–3219. http://dx.doi.org/10.1021/es061812j.